Involvement of ATP synthase residues αArg-376, βArg-182, and βLys-155 in Pi binding

Zulfiqar Ahmad, Alan E. Senior*

Department of Biochemistry and Biophysics, Box 712, University of Rochester Medical Center, Rochester NY 14642, USA

Received 2 November 2004; revised 1 December 2004; accepted 6 December 2004

Available online 21 December 2004

Edited by Stuart Ferguson

Abstract αArg-376, βLys-155, and βArg-182 are catalytically important ATP synthase residues that were proposed to be involved in substrate Pi binding and subsequent steps of ATP synthesis [Senior, A.E., Nadanaciva, S. and Weber, J. (2002) Biochim. Biophys. Acta 1553, 188–211]. Here, it was shown using purified *Escherichia coli* F_1-ATPase that whereas Pi protected wild-type from reaction with 7-chloro-4-nitrobenzo-2-oxa-1,3-diazole, mutations βK155Q, βR182Q, βR182K, and αR376Q abolished protection. Therefore, in ATP synthesis initial binding of substrate Pi in open catalytic site βE is supported by each of these three residues.

Keywords: Oxidative phosphorylation; ATP synthase; ATP synthesis mechanism; Catalytic site βE; Pi binding residue

1. Introduction

ATP synthase is the enzyme responsible for ATP synthesis in oxidative and photo-phosphorylation in eukaryotes and prokaryotes, and for ATP-dependent formation of a transmembrane gradient of protons (or Na^+ ions) in prokaryotes under anaerobic conditions. The enzyme from *Escherichia coli* represents the simplest structural example and consists of the membrane-extrinsic F_1 sector (subunits $\alpha_3\beta_3\gamma\delta\varepsilon$) and the membrane-associated F_o sector (subunits ab_2c_{10}). X-ray structures of bovine enzyme [1] established the presence of three catalytic sites at α/β subunit interfaces of the $\alpha_3\beta_3$ hexamer in the F_1 sector. An important feature of the mechanism is that one group of subunits (the ''rotor'' made up of $\gamma\varepsilon c_{10}$) undergoes rapid, continuous, 360° rotation as catalysis proceeds [2]. In the direction of ATP-driven proton transport, sequential ATP hydrolysis at the three catalytic sites generates rotation of γ, and rotation of the connected c_{10} ring against the *a* subunit moves protons outward across the membrane. A ''stator'' made up of $b_2\delta$ subunits prevents co-rotation of catalytic sites and *a* subunit with the rotor. Conversely, during oxidative phosphorylation, rotation is in the opposite direction and generates ATP [3,4]. Recent reviews of ATP synthase structure and function may be found in [5,6].

The reaction mechanisms of ATP hydrolysis and synthesis and their relationship to mechanical rotation in this molecular nanomotor are therefore of topical interest. In recent work, our laboratory has studied Pi binding, for two reasons. First, it was shown [7–9] that Pi binding is ''energy-linked'', implying that it is linked directly to subunit rotation. Second, as an explanation of how the enzyme binds ADP into catalytic sites during ATP synthesis against apparently prohibitive cellular ATP/ADP concentration ratios, we proposed [10] that rotation-linked binding of Pi occurs first and thereby allows ADP binding while sterically preventing ATP binding. Perez et al. [11] using bovine enzyme showed that Pi protected from inhibition by 7-chloro-4-nitrobenzo-2-oxa-1,3-diazole (NBD-Cl) and Orriss et al. [12] showed by X-ray crystallography that NBD-Cl reacts specifically in catalytic site βE. Together, this information provides an assay for initial binding of substrate Pi in site βE in ATP synthesis. We found that Pi protected wild-type *E. coli* F_1 from NBD-Cl reaction and that mutagenesis of residue βArg-246 [1] to Ala, Gln or Lys abolished Pi protection [13]. Thus, consistent with its charge and location 4.5 Å from the SO_4^{2-} anion in the βADP + Pi catalytic site [14], residue β-Arg-246 was shown to be a Pi binding residue.

Based on fluorimetric assays of MgATP, MgADP, and transition state analog binding in mutant enzymes, and utilizing X-ray structure information, we presented previously a proposal for the molecular mechanism of ATP synthesis [15]. We focussed on three critical catalytic site residues, namely βLys-155 (of the Walker A sequence), βArg-182 and αArg-376, invoking roles for each in Pi binding/release, transition state stabilization, and MgATP binding/release. However, relevant measurements of Pi binding had not been reported. Here, we assayed Pi binding in catalytic site βE by measuring protection from NBD-Cl reaction in αR376Q, αR376K, βK155Q, βR182Q, and βR182K mutant enzymes. The data yield additional support for our proposal regarding ATP synthase reaction mechanism.

2. Materials and methods

2.1. Purification of F_1; depletion of catalytic-site bound nucleotide; assay of ATPase activity of purified F_1

F_1 was purified as in [16]. Prior to the experiments, F_1 samples (100 μl) were passed twice through 1 ml centrifuge columns (Sephadex G-50) equilibrated in 50 mM Tris–SO_4, pH 8.0, to remove catalytic site-bound nucleotide [17]. Catalytic-site bound nucleotide was assayed using the quench of fluorescence (λ_{exc} = 295 nm, λ_{em} = 360 nm) of the

*Corresponding author. Fax: +1 585 271 2683.
E-mail address: alan_senior@urmc.rochester.edu (A.E. Senior).

Abbreviations: NBD-Cl, 7-chloro-4-nitrobenzo-2-oxa-1,3-diazole; DTT, dithiothreitol; MgADP–BeF_x, complex of MgADP and beryllium fluoride

[1] *E. coli* residue numbers used throughout.

0014-5793/$22.00
doi:10.1016/j.febslet.2004.12.022

specific probe βTrp-331, present in all the mutant enzymes. As established previously [18], addition of saturating (2 mM) MgATP or MgADP to enzyme with empty catalytic sites yields 51% quench of β-Trp331 fluorescence. Using this technique it was found that the mutant enzyme preparations, after passage through two centrifuge columns as above, contained ⩽0.2 mol/mol of catalytic site bound nucleotide. ATPase activity was measured in 1.0 ml assay buffer containing 10 mM NaATP, 4 mM $MgCl_2$, and 50 mM Tris–SO_4, pH 8.5, at 37 °C. Reactions were started by addition of enzyme and stopped by addition of SDS to 3.3% final concentration. Pi was assayed as in [19]. For wild-type F_1, reaction times were 2–5 min, with 5–20 μg. For mutant enzymes, reaction times were 30–120 min, using 20–100 μg. All reactions were shown to be linear with time and protein concentration.

2.2. E. coli strains

Wild-type strain SWM1 was used [20]. Mutant strains were αR376Q/βY331W and αR376K/βY331W [21], βR182Q/βY331W and βR182K/βY331W [22], and βK155Q/βY331W [23]. All these enzymes contained the βY331W mutation to make them compatible with previous work involving fluorimetric estimations of nucleotide binding and transition state formation and to allow calculation of catalytic-site bound nucleotide as in Section 2.1 above [18,21–25]. The βY331W mutation by itself does not significantly affect activity.

2.3. Inhibition of ATPase activity

For NBD-Cl inhibition of purified F_1, enzyme (0.2–1.0 mg/ml) was reacted with NBD-Cl for 60 min in the dark, at 23 °C, in 50 mM Tris–SO_4, pH 8.0, and 2.5 mM $MgSO_4$, then 50 μl aliquots were transferred to 1.0 ml of ATPase assay buffer. Where protection from NBD-Cl inhibition was determined, F_1 was preincubated 60 min with MgADP or Pi before addition of NBD-Cl. Control samples contained ligand without added NBD-Cl. Neither Pi (up to 50 mM) nor MgADP (up to 10 mM) had any inhibitory effect alone.

Table 1
ATPase activity of mutant F_1 enzymes

F_1 species	Specific ATPase activity (μmol/min/mg)
Wild-type	42.0
βK155Q	0.023 (1830×)
βR182K	0.250 (168×)
βR182Q	0.020 (2100×)
αR376K	0.120 (350×)
αR376Q	0.025 (1680×)

Results are means of 15–20 replicates which agreed ±10%. Numbers in parentheses indicate reduction in activity caused by the mutation.

3. Results

3.1. ATPase activity of F_1 enzymes containing mutations at residues βLys-155, βArg-182, and αArg-376

Table 1 shows specific ATPase activity of mutant enzymes measured at 37 °C. Each of these mutations had been shown previously to strongly impair both ATP synthesis in cells and ATP hydrolysis in purified enzyme, so it was not surprising that the activities shown in Table 1 were very low indeed. However, this was the first time the specific ATPase activities had been determined accurately at elevated temperature with large amounts of enzyme for long incubation periods. Duplicate (in some cases triplicate) preparations of the same mutant enzyme gave the identical specific activity. Each of the enzymes showed the same purity as wild-type when analyzed by SDS-gel electrophoresis. The data show that the activities reported are referable to F_1 and not to contaminants and further data supporting this are given below.

3.2. Reaction of mutant F_1 enzymes with NBD-Cl and reversal by dithiothreitol

Mutant enzymes were first reacted with varied concentrations of NBD-Cl for 1 h at 23 °C, then assayed for ATPase activity (Fig. 1). Surprisingly, both βK155Q (Fig. 1A) and βR182Q (Fig. 1B) showed activation of ATPase by NBD-Cl; whereas in wild-type (Fig. 1C, *open circles*), potent inhibiton occurred consistent with many previous studies. Mutants βR182K, αR376K and αR376Q were inhibited by NBD-Cl, albeit to differing degree and in each case less than in wild-type (Fig. 1C). As Fig. 1C shows, increasing the concentration of NBD-Cl in the preincubation above 100 μM did not result in further inhibition. To be sure that maximal reaction with NBD-Cl had been reached, we incubated each enzyme with 150 μM NBD-Cl for 1 h as in Fig. 1, then added a further pulse equivalent to 200 μM NBD-Cl and continued incubation for a further hour before assaying ATPase. There was no further decrease in activity of βR182K, αR376K or αR376Q enzymes, showing that in these cases reaction was complete and that the fully reacted enzyme retained residual activity. With βK155Q and βR182Q enzymes, further activation was seen, to the degree expected from Fig. 1A and B. When wild-type

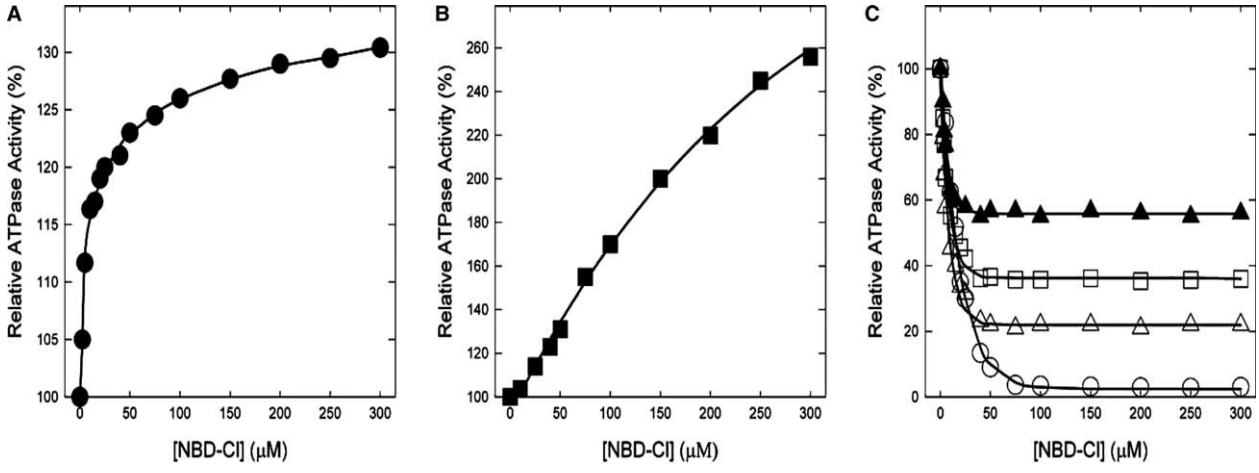

Fig. 1. Reaction of mutant and wild-type enzymes with NBD-Cl. F_1 was reacted with varied concentrations of NBD-Cl as shown for 1 h in the dark at 23 °C, then aliquots of reacted enzyme were assayed for ATPase activity. Further details are given in Section 2. Note that the vertical axes are different in panels A, B, and C. ●, βK155Q; ■, βR182Q; □, βR182K; Δ, αR376K; ▲, αR376Q; and ○, wild-type. Results are means of quadruplicate experiments which agreed within ±10%.

and mutant enzymes were preincubated with 125 μM NBD-Cl as in Fig. 1, then 4 mM dithiothreitol (DTT) was added and incubation continued for 1 h before assay of ATPase, it was seen that DTT completely reversed the effect of NBD-Cl (data not shown). In wild-type enzyme, it was shown that NBD-Cl reacts specifically with residue βTyr-297 and that incubation with DTT removes reacted NBD and restores activity [26,27]. Thus, NBD-Cl is reacting with residue βTyr-297 in mutant F_1 to produce the effects seen.

3.3. Protection against NBD-Cl reaction by MgADP or Pi

We previously found that MgADP protected against NBD-Cl reaction in wild-type enzyme, but only at high concentrations (EC_{50} ~4 mM [13]), consistent with the conclusion of Orriss et al. [12] that NBD-Cl reacts specifically in the βE catalytic site. Here, we showed that the reaction of NBD-Cl with mutant enzymes was protected by MgADP (Fig. 2) with EC_{50} approximately the same in mutants and wild-type. From this we may conclude that NBD-Cl is reacting in the βE site in the mutants, and that the activities measured are due to F_1 and not due to a contaminant.

Protection against NBD-Cl reaction by Pi is shown in Fig. 3. *Open circles* represent reaction of F_1 (wild-type or mutant) with NBD-Cl in the absence of Pi, *open squares* represent reaction in the presence of 2.5 mM Pi, and *open triangles* represent reaction in the presence of 10 mM Pi. Wild-type is shown in Fig. 3A. The results show that Pi protects well confirming previous data [11,13]. Fig. 3B–D show mutants βK155Q, βR182K and βR182Q, respectively. It is evident that all three mutations abolish the ability of Pi to protect, demonstrating that residues βLys-155 and βArg-182 are required for Pi binding in wild-type. The substitution of Lys for Arg at residue β-182 is not sufficient to support Pi binding, apparently. Figs. 3E and F show αR376K and αR376Q, respectively. Protection is seen in the Lys mutant but not in the Gln mutant. From the Gln mutant result, we conclude that αArg-376 is involved in Pi binding in wild-type; apparently, the Lys mutant can substitute for Arg in carrying out Pi binding.

4. Discussion

Mutagenesis and X-ray structural analyses of F_1, the catalytic sector of ATP synthase, had identified three basic residues within catalytic sites as critical for catalysis, namely βLys-155 (of the Walker A sequence), βArg-182 and αArg-376. We earlier reported MgATP and MgADP binding parameters in mutant enzymes αR376K, αR376Q, βK155Q, βR182K and βR182Q by fluorimetric analyses using introduced βTrp-331 as specific catalytic site probe, and analyses of transition state formation using MgADP–fluoroaluminate and MgADP–fluoroscandium as transition state analogs [21–25]. Missing from these analyses was a direct measurement of Pi binding in the mutant enzymes. Such assays are presented in this paper.

The βK155Q mutant lacks ATP synthesis [23] and has very low F_1-ATPase activity (Table 1). Previous work had shown that residue βLys-155 plays a major role in binding MgATP, particularly at catalytic sites of high and medium nucleotide affinity, but not in binding MgADP [23]. βLys-155 is also critical for transition state formation [24,25]. X-ray structures of native F_1 with MgAMPPNP and MgADP bound [1], of MgADP–BeF_x inhibited F_1 [28], of MgADP–AlF_4^- inhibited F_1 representing the transition state [14], and of MgADP–AlF_3 inhibited F_1 representing the late transition state/early ground state [29] all show the ε-amino group of βLys-155 very close (⩽3 Å) to the γ-phosphate position, consistent with the

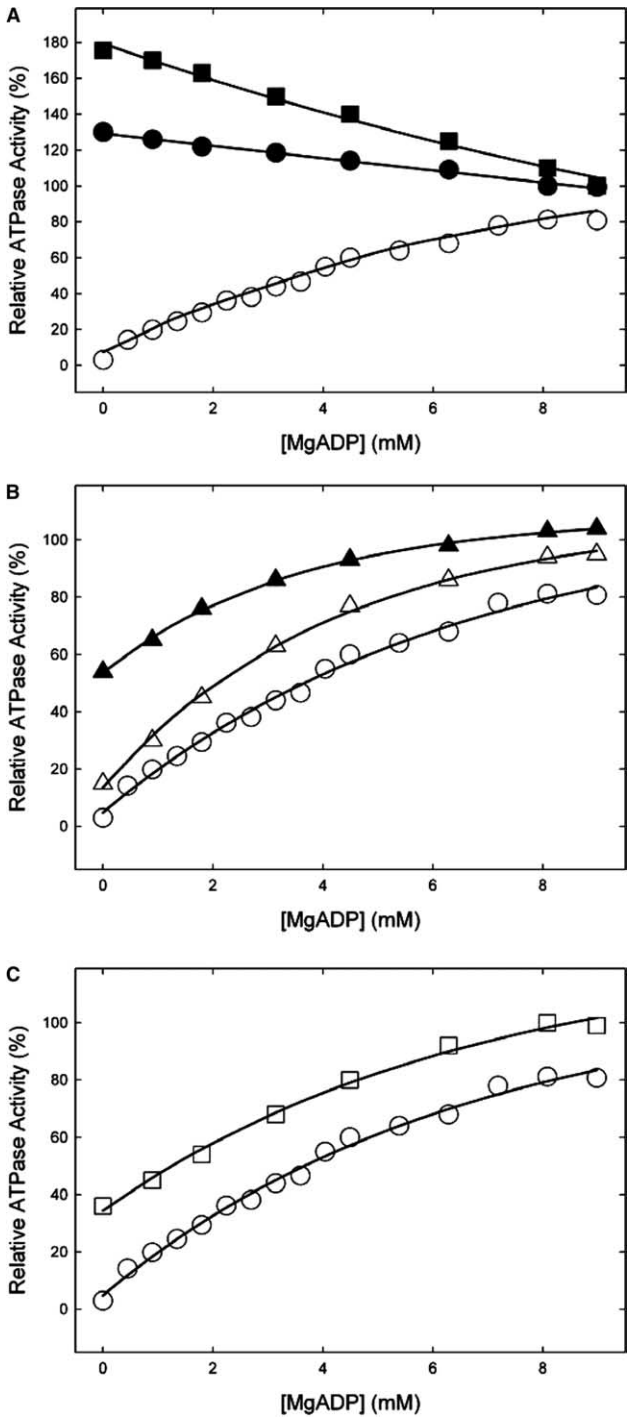

Fig. 2. Protection against NBD-Cl reaction by MgADP. Wild-type and mutant enzymes were preincubated for 1 h at room temperature with varied concentrations of MgADP as shown, then 125 μM NBD-Cl was added and incubation continued at room temperature in the dark for 1 h. Aliquots were then assayed for ATPase activity. Note that the vertical axis in panel A is different to B, C. ●, K155Q; ■, βR182Q; □, βR182K; Δ, αR376K; ▲, αR376Q; and ○, wild-type. Results are means of quadruplicate experiments which agreed within ±10%.

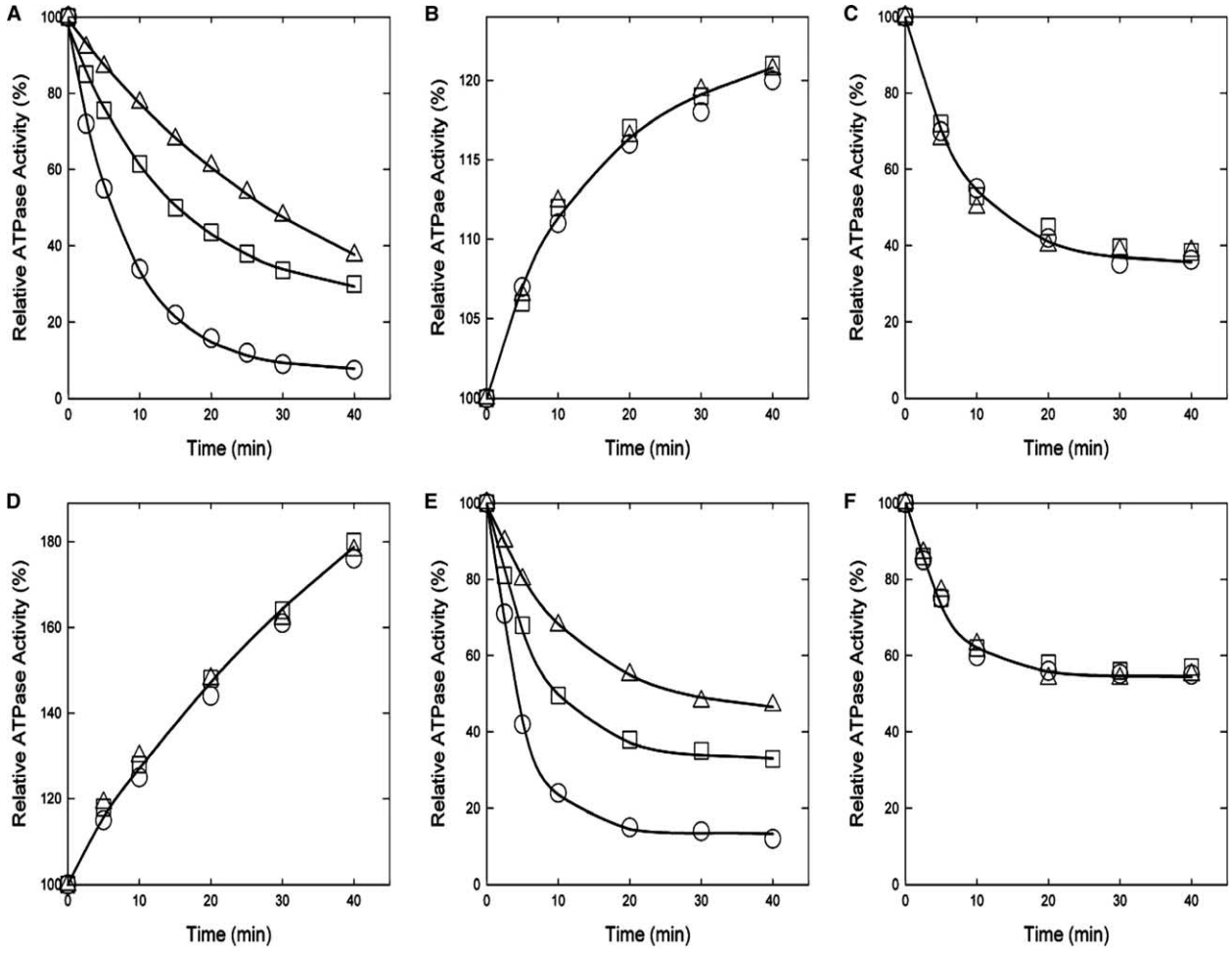

Fig. 3. Protection against NBD-Cl reaction by Pi. Wild-type and mutant enzymes were preincubated with Pi for 1 h at room temperature, then 100 μM NBD-Cl was added. Aliquots were withdrawn at time intervals shown for ATPase assay. ATPase activity remaining is plotted against time of incubation with NBD-Cl. (A) Wild-type; (B) βK155Q; (C) βR182K; (D) βR182Q; (E) αR376K; and (F) αR376Q. ○, no Pi added; □, 2.5 mM Pi; Δ, 10 mM Pi. Results are means of quadruplicate experiments which agreed within ±10%.

above conclusions. We had hypothesized further that βLys-155 was important for Pi binding in ATP synthesis [15]. This was experimentally confirmed in this work by the data in Fig. 3B, showing that Pi binding in the βE catalytic site is abolished in βK155Q. Therefore, residue βLys-155 is involved at all stages of ATP synthesis from Pi binding through the transition state to MgATP formation.

Mutants βR182Q and βR182K lack ATP synthesis activity [22] and have low F_1-ATPase (Table 1). Residue βArg-182 had been shown to be involved in MgATP binding at the site of highest affinity [22] but not in MgADP binding. Transition state formation is abolished by βR182Q but retained in βR182K [22]. In this regard it may be noted that βR182K F_1 did have somewhat higher ATPase activity (Table 1). We had hypothesized that βArg-182 is required for Pi binding in ATP synthesis [15], this was confirmed by data in Fig. 3C and D, where both βR182Q and βR182K mutations abolished Pi binding in site βE. Therefore, residue βArg-182 is also involved at all stages of ATP synthesis from Pi binding through ATP formation.

Following the G-protein literature, we earlier applied the term "arginine finger" to describe residue αArg-376, based on the findings that it was a required ligand for the catalytic transition state but was not involved in MgATP or MgADP binding [21], this despite its apparent proximity to the γ-phosphate of MgAMPPNP in X-ray structures. [2] Movement of this residue in and out of the catalytic site was inferred, and was postulated to produce the rate acceleration (positive catalytic cooperativity) linked to subunit rotation and full (tri-site) catalytic site occupancy that is a hallmark of the mechanism [15]. Significant spatial displacements of residue αArg-376 have been noted in X-ray structures representing different reaction intermediates [1,14,28–30] and it was discussed that conformational freedom of this residue likely contributes to its importance in catalysis [28].

We had hypothesized a role for this residue in Pi binding in ATP synthesis [15] and this was confirmed here by Fig. 3F in which Pi failed to protect αR376Q F_1 from NBD-Cl inhibition.

[2] A recent X-ray structure [28] showed that bound MgADP–BeF_x mimicked bound MgATP. In assays of F_1-ATPase we found that wild-type and αR376Q were fully inhibited by MgADP plus BeF_x, whereas βK155Q and βR182Q were fully resistant (Ahmad, Z., and Senior, A.E., unpublished work), supporting that βLys-155 and βArg-182 are MgATP ligands but αArg-376 is not. Stringent stereochemical orientation factors may play a role in determining functional interactions of αArg-376.

However, just as αR376K mutant was able to form the transition state [21], so it was also able to support Pi binding (Fig. 3E). It is nevertheless strongly impaired in both ATP synthesis and hydrolysis, emphasizing that this residue has other required function(s), likely in conformational movements or in H-bonding to other side-chains, that are specific to Arg and not supported by Lys.

In the assays of Pi binding presented here, no nucleotide was present and enzymes were prepared so as to have all three catalytic sites essentially empty (see Section 2.1). The sites would therefore be in conformation βE. In this conformation [29], αArg-376 and βArg-246 (identified in [13] as a Pi-binding residue) lie 2.6 and 4.0 Å from βArg-182, whereas βLys-155 lies 9.5, 7.3, and 6.3 Å from αArg-376, βArg-182 and βArg-246, respectively. In essence the four residues form a triangle, with βLys-155 at the apex and αArg-376, βArg-182 and βArg-246 along the base. A potential Pi-binding pocket can readily be envisaged at the center of the triangle. In ATP synthesis, the βE site will change to the β ADP + Pi (half-closed) site in association with γ-rotation [14,15]. The X-ray structure of this conformation [14] shows that each of the residues αArg-376, βLys-155 and βArg-182 is located $\leqslant$3.0 Å from the nearest oxygen atom of bound SO_4^{2-} anion (thought to represent Pi), whereas βArg-246 is 4.5 Å from the sulfate. Thus, as the reaction proceeds the three residues αArg-376, βLys-155 and βArg-182 close around the Pi and move it away from βArg-246 toward the site of transition state formation, consistent with [15].

Summarizing, data presented here support a proposed molecular mechanism for ATP synthesis [15]. Initially, substrate Pi binds in the βE catalytic site using four basic residues as ligands, namely the three described in this paper, αArg-376, βArg-182 and βLys-155, plus βArg-246 as described in [13]. After binding of MgADP (in which these four residues are not involved), the catalytic transition state forms, using αArg-376, βArg-182 and βLys-155 as direct ligands. Upon formation of MgATP, αArg-376 withdraws and no longer interacts, whereas βLys-155 and βArg-182 are still liganded to the γ-phosphate. Release of MgATP to the medium involves breaking these ligands. Ligands to the Mg^{2+} cation [30,31] are βThr-156 (direct), βGlu-185 and βAsp-242 (both via water molecules), which are also critical for the reaction. In the foregoing we have discussed only ligands involved directly in liganding Pi, the pentavalent phosphate of the catalytic transition state, and the γ-phosphate of MgATP. Sequential, rotation-dependent utilization of catalytic sites (βE, βADP + Pi, βTP, and βDP) in ATP synthase means that different steps of the reaction mechanism occur in temporal succession in distinct conformations of the catalytic sites. This was discussed previously by our laboratory in [15] and an excellent recent discussion may be found in [28].

Acknowledgement: This work was supported by NIH Grant GM25349 to AES.

References

[1] Abrahams, J.P., Leslie, A.G.W., Lutter, R. and Walker, J.E. (1994) Structure at 2.8 Å resolution of F_1-ATPase from bovine heart mitochondria. Nature 370, 621–628.
[2] Noji, H., Yasuda, R., Yoshida, M. and Kinosita, K. (1997) Direct observation of the rotation of F_1-ATPase. Nature 386, 299–302.
[3] Diez, M., Zimmerman, B., Börsch, M., König, M., Schweinberger, E., Steigmiller, S., Reuter, R., Felekyan, S., Kudryavtsev, V., Seidel, P. and Gräber, P. (2004) Proton-powered subunit rotation in single membrane-bound F_oF_1-ATP synthase. Nat. Struct. Mol. Biol. 11, 135–141.
[4] Itoh, H., Takahashi, A., Adachi, K., Noji, H., Yasuda, R., Yoshida, M. and Kinosita, K. (2004) Mechanically driven ATP synthesis by F_1-ATPase. Nature 427, 465–468.
[5] Noji, H. and Yoshida, M. (2001) The rotary machine in the cell, ATP synthase. J. Biol. Chem. 276, 1665–1668.
[6] Weber, J. and Senior, A.E. (2003) ATP synthesis driven by proton transport in F_1F_o-ATP synthase. FEBS Lett. 545, 61–70.
[7] Boyer, P.D. (1989) A perspective of the binding change mechanism for ATP synthesis. FASEB J. 3, 2164–2178.
[8] Al-Shawi, M.K. and Senior, A.E. (1992) Effects of dimethyl sulfoxide on catalysis in *Escherichia coli* F_1-ATPase. Biochemistry 31, 886–891.
[9] Al-Shawi, M.K., Ketchum, C.J. and Nakamoto, R.K. (1997) The *Escherichia coli* F_oF_1 γM23K uncoupling mutant has a higher $K_{0.5}$ for Pi. Transition state analysis of this mutant and others reveals that synthesis and hydrolysis utilize the same kinetic pathway. Biochemistry 36, 12961–12969.
[10] Weber, J. and Senior, A.E. (2000) ATP synthase: what we know about ATP hydrolysis and what we do not know about ATP synthesis. Biochim. Biophys. Acta 1458, 300–309.
[11] Perez, J.A., Greenfield, A.J., Sutton, R. and Ferguson, S.J. (1986) Characterisation of phosphate binding to mitochondrial and bacterial membrane-bound ATP synthase by studies of inhibition with 4-chloro-7-nitrobenzofurazan. FEBS Lett. 198, 113–118.
[12] Orriss, G.L., Leslie, A.G.W., Braig, K. and Walker, J.E. (1998) Bovine F_1-ATPase covalently inhibited with 4-chloro-7-nitrobenzofurazan: the structure provides further support for a rotary catalytic mechanism. Structure 6, 831–837.
[13] Ahmad, Z. and Senior, A.E. (2004) Mutagenesisn of residue βArg-246 in the phosphate-binding subdomain of catalytic sites of *Escherichia coli* F_1-ATPase. J. Biol. Chem. 279, 31505–31513.
[14] Menz, R.I., Walker, J.E. and Leslie, A.G.W. (2001) Structure of bovine mitochondrial F_1-ATPase with nucleotide bound to all three catalytic sites: Implications for the mechanism of rotary catalysis. Cell 106, 331–341.
[15] Senior, A.E., Nadanaciva, S. and Weber, J. (2002) The molecular mechanism of ATP synthesis by F_1F_o-ATP synthase. Biochim. Biophys. Acta 1553, 188–211.
[16] Weber, J., Lee, R.S.F., Grell, E., Wise, J.G. and Senior, A.E. (1992) On the location and function of tyrosine β331 in the catalytic site of *Escherichia coli* F_1-ATPase. J. Biol. Chem. 267, 1712–1718.
[17] Weber, J., Wilke-Mounts, S. and Senior, A.E. (1994) Cooperativity and stoichiometry of substrate binding to the catalytic sites of *Escherichia coli* F_1-ATPase. Effects of magnesium, inhibitors and mutation. J. Biol. Chem. 269, 20462–20467.
[18] Weber, J. and Senior, A.E. (2004) Fluorescent probes applied to catalytic cooperativity in ATP synthase. Methods Enzymol. 380, 132–152.
[19] Taussky, H.H. and Shorr, E. (1953) A microcolorimetric method for the determination of inorganic phosphorus. J. Biol. Chem. 202, 675–685.
[20] Rao, R., Al-Shawi, M.K. and Senior, A.E. (1988) Directed mutagenesis of the strongly conserved lysine 175 in the proposed nucleotide-binding domain of α-subunit from *Escherichia coli* F_1-ATPase. J. Biol. Chem. 263, 5569–5573.
[21] Nadanaciva, S., Weber, J., Wilke-Mounts, S. and Senior, A.E. (1999) Importance of F_1-ATPase residue α-Arg-376 for catalytic transition state stabilization. Biochemistry 38, 15493–15499.
[22] Nadanaciva, S., Weber, J. and Senior, A.E. (1999) The role of β-Arg-182, an essential catalytic residue in *Escherichia coli* F_1-ATPase. Biochemistry 38, 7670–7677.
[23] Löbau, S., Weber, J., Wilke-Mounts, S. and Senior, A.E. (1997) F_1-ATPase, roles of three catalytic site residues. J. Biol. Chem. 272, 3648–3656.
[24] Nadanaciva, S., Weber, J. and Senior, A.E. (1999) Binding of the transition state analog MgADP–fluoroaluminate to F_1-ATPase. J. Biol. Chem. 274, 7052–7058.
[25] Nadanaciva, S., Weber, J. and Senior, A.E. (2000) New probes of the F_1-ATPase catalytic transition stat reveal that two of the three catalytic sites can assume a transition state conformation simultaneously. Biochemistry 39, 9583–9590.

[26] Ferguson, S.J., Lloyd, W.J., Lyons, M.H. and Radda, G.K. (1975) The mitochondrial ATPase. Evidence for a single essential tyrosine residue. Eur. J. Biochem. 54, 117–126.
[27] Sutton, R. and Ferguson, S.J. (1985) Tyrosine-311 of a β chain is the essential residue specifically modified by 4-chloro-7-nitrobenzofurazan in bovine heart mitochondrial ATPase. Eur. J. Biochem. 148, 551–554.
[28] Kagawa, R., Montgomery, M.G., Braig, K., Leslie, A.G.W. and Walker, J.E. (2004) The structure of bovine F_1-ATPase inhibited by ADP and beryllium fluoride. EMBO J. 23, 2734–2744.
[29] Braig, K., Menz, R.I., Montgomery, M.G., Leslie, A.G.W. and Walker, J.E. (2000) Structure of bovine F_1-ATPase inhibited by MgADP and aluminium fluoride. Structure 8, 567–573.
[30] Gibbons, C., Montgomery, M.G., Leslie, A.G.W. and Walker, J.E. (2000) The structure of the central stalk in bovine F_1-ATPase at 2.4 Å resolution. Nature Struct. Biol. 7, 1055–1061.
[31] Weber, J., Hammond, S.T., Wilke-Mounts, S. and Senior, A.E. (1998) Mg^{2+} coordination in catalytic sites of F_1-ATPase. Biochemistry 37, 608–614.